Manipulating the asymmetry of magnetization reversal in epitaxial CoO/Co films

Hao-Liang Liu,[1] Steven Brems,[3] Yu-Jia Zeng,[1,*] Kristiaan Temst,[2] André Vantomme,[2] and Chris Van Haesendonck[1,†]

[1]*Laboratorium voor Vaste-Stoffysica en Magnetisme, KU Leuven, Celestijnenlaan 200 D, BE-3001 Leuven, Belgium*

[2]*Instituut voor Kern- en Stralingsfysica, KU Leuven, Celestijnenlaan 200 D, BE-3001 Leuven, Belgium*

[3]*Imec vzw, Kapeldreef 75, 3001 Leuven, Belgium*

(Received 27 August 2014; revised manuscript received 29 October 2014; published 1 December 2014)

We investigated the training effect and magnetization reversal in CoO/Co bilayer films grown epitaxially on MgO (001) substrates. The asymmetry of the magnetization reversal, which appears due to the exchange bias after field cooling, survives after training, in contrast to the case of polycrystalline bilayers. By applying hysteresis loops with the magnetic field perpendicular to the cooling field, we are able to modify the orientation of the average uncompensated magnetization of the antiferromagnetic CoO. Subsequently, the untrained state can be partially restored, and more importantly the magnetization reversal asymmetry can be inverted by starting the perpendicular loop with the appropriate field polarity. Consequently, we succeeded in manipulating the magnetization reversal asymmetry and even in achieving opposite reversal asymmetries in the same exchange bias system.

DOI: 10.1103/PhysRevB.90.214402 PACS number(s): 75.60.Jk, 75.47.−m

The interfacial coupling between ferromagnetic (FM) and antiferromagnetic (AF) spin structures, known as the exchange bias (EB) effect, gives rise to a shift and/or a broadening of the hysteresis loop [1–3]. Although EB has been widely applied in spintronic devices, the underlying physical mechanism remains a highly debated issue [4]. Many peculiar properties have been observed in different EB systems [5–9], including training effect (decrease of pinning upon consecutive field cycling) [10–13] and asymmetry of magnetization reversal (different reversal mechanisms on descending and ascending branches of the same hysteresis loop) [5,13,14].

The training effect and the asymmetry of the magnetization reversal have been extensively investigated by polarized neutron reflectometry [5,6,13,15], vibrating sample magnetometry [16], anisotropic magnetoresistance (AMR) [7,12], vectorial Kerr magnetometry [17], and magnetic domain imaging [18]. In the polycrystalline CoO/Co bilayer system, the magnetization reversal is governed by domain wall motion in the descending branch and by magnetization rotation in the ascending branch in the first hysteresis loop after field cooling (FC), and only magnetization rotation remains present in both branches after training [11,19]. Different and even opposite scenarios have been reported for other EB systems, e.g., coherent rotation of magnetization in the descending branch and domain wall motion in the ascending branch in Fe/FeF_2 and Fe/MnF_2 [5,20]. Hoffmann indicated that the higher order symmetry of the AF layer can play a key role in the training effect [21]. Based on the Fulcomer and Charap model, the training effect can be explained as a result of spin reorientation of the uncompensated AF grains [11,22]. Radu *et al.* reported that the training effect and reversal asymmetry may be attributed to the formation of interfacial domains with domain wall parallel to the interface [13]. Camarero *et al.* have linked the asymmetry to competing anisotropies within the coherent rotation model [14]. Experimental results and simulations also indicate that the asymmetric reversal can be related to the higher order FM anisotropy [5], domain wall formation perpendicular to the interface in the AF layer [23], finite-size effect of AF grains [24], and the intrinsic broken symmetry [25]. Since the microscopic origin of the reversal asymmetry and training is still elusive, additional experiments are needed to identify the underlying physical mechanisms.

We reported previously on the exciting possibility to largely restore the untrained state in polycrystalline CoO/Co by performing a hysteresis loop perpendicular to the FC direction with the appropriate field amplitude limited to a small range, without warming up the system above the Néel temperature [19,26]. Here, we investigate the training effect and reversal asymmetry in the epitaxially grown CoO/Co system for which the interplay between magnetocrystalline anisotropy (MCA) and the EB effect can be studied. The presence of MCA results in survival of the reversal asymmetry after training and also after applying perpendicular hysteresis loops. The magnetization reversal asymmetry can be inverted with the appropriate field amplitude for the perpendicular hysteresis loops. Thus we demonstrate the possibility to manipulate the magnetization reversal asymmetry. Moreover, a substantial positive EB appears in the perpendicular loops. We only focus on the training effect and reversal asymmetry along the hard axis of the FM layer, since the domain wall motion mechanism due to the MCA overwhelms the influence of the EB effect for FC along the easy axis [27]. The details of the magnetization reversal are revealed by the experimental results of four-probe high-resolution anisotropic magnetoresistance (AMR) measurements. The AMR value depends on the magnetization direction with respect to the current direction, and can be expressed as $R(\theta) = R_{\perp} + \triangle R_0 \cos^2\theta$, where θ is the angle between magnetization and current, $R_{\perp}$ is the resistance with magnetization perpendicular to the current, and $\triangle R_0$ is the difference of resistance between magnetization parallel and perpendicular to the current.

Co films were grown by molecular beam epitaxy on MgO (001) oriented substrates. Prior to the growth the substrate is annealed at 600 °C for 1 h to remove adsorbed gases from the surface. Subsequently the substrate was cooled down to the deposition temperature of 300 °C and a 5 nm Co

*yujia.zeng@fys.kuleuven.be

†chris.vanhaesendonck@fys.kuleuven.be

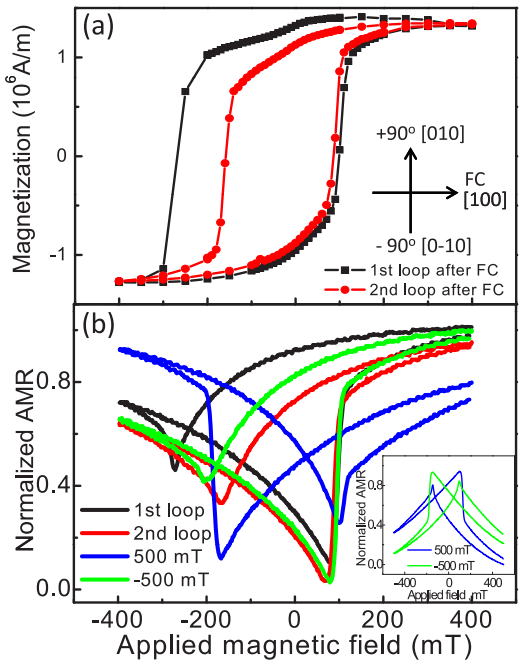

FIG. 1. (Color online) (a) Two subsequent hysteresis loops after FC from room temperature to 10 K along MgO [100] measured by SQUID magnetometry. Inset: the definition of the applied field directions in the measurement. (b) AMR measurements of the corresponding hysteresis loops of (a) and the restored hysteresis loops along cooling field after perpendicular loops. Inset: perpendicular hysteresis loops with field amplitudes of 500 mT and −500 mT.

film is deposited at a rate of 0.49 nm/min. After deposition the film was oxidized *in situ* in a partial oxygen atmosphere of 10^{-3} mbar for 2 min, which results in the formation of a CoO top layer with thickness 2–3 nm [7]. The surface morphology of the Co film after oxidation was characterized by *in situ* scanning tunneling microscopy (STM), indicating an average rms roughness below 0.8 nm. X-ray diffraction (XRD) identified the Co $(11\bar{2}0)_{hcp}$ structure on MgO (001), in agreement with Ref. [28]. The in-plane fourfold symmetry was confirmed by measurement of the magnetic anisotropy using magneto-optic Kerr magnetometry. The magnetic anisotropy has fourfold symmetry with hard axis along ⟨100⟩ and easy axis along ⟨110⟩, with a superimposed small uniaxial magnetic anisotropy with easy axis along $[\bar{1}10]$. EB was established by magnetic field cooling in 400 mT along [100] from room temperature to 10 K.

Figure 1(a) presents the two subsequent hysteresis loops measured by superconducting quantum interference device (SQUID) magnetometry at 10 K with field applied parallel to the FC direction. Both the coercivity and the EB (shift of the hysteresis loop) considerably change in the second hysteresis loop due to the training effect. The first magnetization reversal after FC is much more rounded than in polycrystalline CoO/Co due to the influence of MCA [13,26]. The reversal asymmetry, which does not appear very pronounced in magnetization measurements, is more clearly reflected by the AMR results in Fig. 1(b). The variation of the AMR is obviously smaller in the descending branch than in the ascending branch, indicating that magnetization reversal by domain wall motion is more dominating in the descending branch. After training the reversal asymmetry decreases, but clearly survives the training, which is different from its disappearance in polycrystalline films [13,19,26]. The EB field and reversal asymmetry in the subsequently trained hysteresis loops are close to those in the second hysteresis loop.

It is important to note that the AMR measurements in Fig. 1(b) indicate that the ferromagnetic magnetization at the highest positive fields is reduced after going through a complete hysteresis loop. As discussed in detail below, this small but finite reduction originates from a rearrangement of the average uncompensated antiferromagnetic magnetization after training, resulting in a ferromagnetic magnetization that becomes rotated away from the field cooling direction. We already reported before on a similar small decrease of the ferromagnetic magnetization for polycrystalline CoO/Co samples [26]. The small decrease of the ferromagnetic magnetization does not appear in the magnetization curves obtained using measurements by SQUID magnetometry [Fig. 1(a)], because we need to subtract from the SQUID magnetometry signal a very strong diamagnetic background signal resulting from the MgO substrate to obtain the hysteresis loops presented in Fig. 1(a). When doing the subtraction we impose that the magnetization loops become closed and this way the small reduction of the ferromagnetic magnetization is not obviously present.

We investigated in detail the possibility to restore the untrained state by applying hysteresis loops with magnetic field perpendicular to the FC direction, as illustrated in the inset of Fig. 1(b). For this purpose the two possible directions for starting the perpendicular hysteresis loop are defined as the positive direction (+90°) and the negative direction (−90°) according to the inset of Fig. 1(a). The restored hysteresis loops along the FC direction after performing a hysteresis loop with the initial field in the +90° and −90° directions and with a field amplitude of 500 mT are presented in Fig. 1(b). The untrained state can be partially reinduced after performing a hysteresis loop starting in the −90° direction. Surprisingly, the reversal asymmetry in the restored loop is inverted after performing a hysteresis loop starting in the +90° direction, i.e., the reversal proceeds with a larger portion of domain wall motion in the ascending branch. The inset of Fig. 1(b) presents the corresponding perpendicular hysteresis loops starting along +90° and −90° directions, where the reversal asymmetry is opposite to the respective hysteresis loops along the FC direction. To the best of our knowledge, opposite magnetization reversal asymmetries have been seldom discovered in the same EB system. Now we discovered the surprising possibility of inverting the reversal asymmetry in the same EB system.

In order to achieve a quantitative analysis and interpretation of our experimental results, we collect in Fig. 2(a) the EB fields and the degrees of asymmetry for the restored as well as for the perpendicular hysteresis loops as a function of the field amplitudes that are used for performing the perpendicular hysteresis loops. The EB field is determined by $H_{EB} = -(H_{c1} + H_{c2})/2$, where H_{c1} and H_{c2} are the coercive fields of the descending branch and the ascending branch, respectively [13]. On the other hand, the degree of asymmetry is defined as the difference in depth of the valleys in the AMR

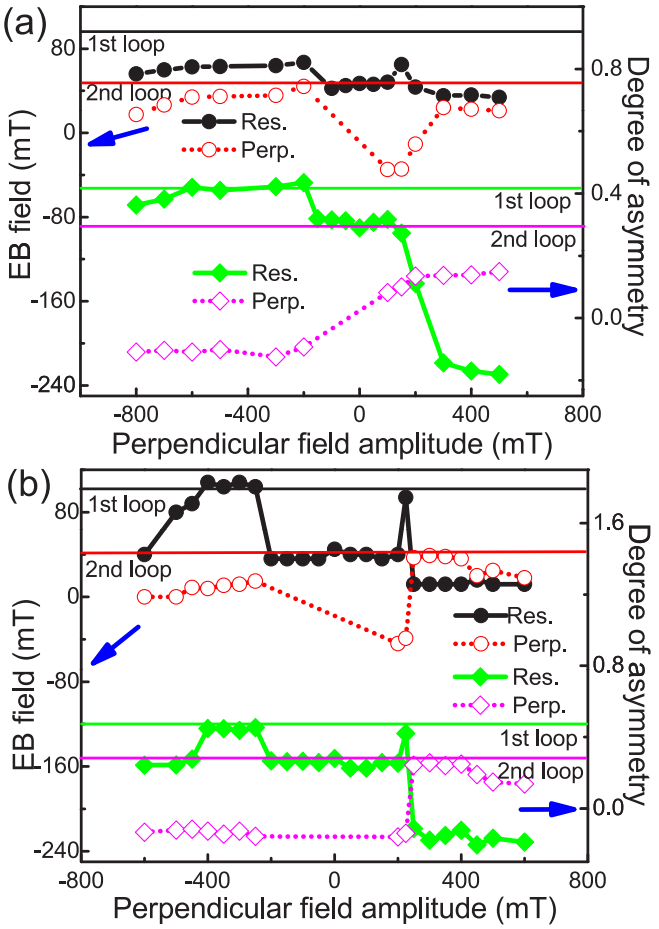

FIG. 2. (Color online) (a) Experimental and (b) simulated dependence of the EB field and degree of asymmetry on the field amplitude of the perpendicular hysteresis loops. Solid and empty dots denote the EB fields of restored and perpendicular hysteresis loops, respectively. The corresponding scale is labeled on the left axis. Solid and empty diamonds denote the degree of asymmetry of restored and perpendicular hysteresis loop, respectively. The corresponding scale is labeled on the right axis. The EB field and degree of asymmetry for the untrained and trained hysteresis loops are indicated by the solid lines for comparison.

curves at the two coercive fields divided by the depth of the AMR valley at the coercive field of the ascending branch [19].

Our main observations in Fig. 2(a) are as follows.

(i) We find that the EB *field of the restored hysteresis loops* becomes in fact smaller after performing a hysteresis loop starting along the $+90^\circ$ direction, except for a field amplitude around 150 mT (see Ref. [19]). This is in contrast to the increase which is observed for all field amplitudes used for the perpendicular hysteresis loops starting along the -90° direction.

(ii) The EB *field of the perpendicular hysteresis loops* reveals a similar trend. However, a quite high "positive EB" (i.e., a negative value of the EB field $H_{\mathrm{EB}} = -34$ mT) appears in the perpendicular loop when the field amplitude is between 100 mT and 250 mT. This is in contrast to previous observations of only a very small value of the positive EB field with $H_{\mathrm{EB}} = -2$ mT [4,8]. Recently, a large positive EB with $H_{\mathrm{EB}} = -13$ mT has also been reported for Co/CoO bilayers within a limited temperature range (around 100 K), where as stated by the authors the effective anisotropy of the AF layer (average uncompensated AF magnetization in our language) reorients in a direction which is far from FC direction [9].

(iii) The *degree of asymmetry of the restored hysteresis loops* gradually decreases and becomes negative when increasing the field amplitude for the perpendicular hysteresis loops starting along the $+90^\circ$ direction, indicating the inversion of the reversal asymmetry. On the other hand, the degree of asymmetry increases and gets close to the value of the untrained state when the field for the perpendicular hysteresis loops starts along the -90° direction.

(iv) The *degree of asymmetry of the perpendicular hysteresis loops* themselves shows the opposite behavior when compared to the respective restored hysteresis loops. We note that the reversal of the asymmetry is present in our perpendicular hysteresis loops as well, which is different from the systems with uniaxial magnetic anisotropy [14,26,29].

Our experimental results can be well explained based on the extended model of Fulcomer and Charap [11,22], which considers many AF grains with size G_i that are exchange coupled with a FM domain with size $\sum G_i$. When adding the MCA term of the FM layer to the total energy, the latter energy can be expressed as

$$E = K_{\mathrm{AF}} t_{\mathrm{AF}} \sum_i G_i \sin^2[2(\alpha_i - \beta_i)] - B \sum_i \sqrt{G_i} \cos(\theta - \alpha_i) + K_F t_F \sin^2\left[2\left(\theta - \frac{\pi}{4}\right)\right] \times \sum_i G_i - \mu_0 H M_S t_F \cos(\varphi - \theta) \sum_i G_i, \quad (1)$$

where $K_{\mathrm{AF}} = 5 \times 10^5$ J/m^3 and $K_F = 0.6 \times 10^5$ J/m^3 are the MCA constants of the AF layer and the FM layer, which both have fourfold symmetry [30]. t_{AF} (3 nm) and t_F (4 nm) represent the thickness of the AF layer and the FM layer. The first term and the third term denote the MCA of the AF layer and of the FM layer, respectively. The second term is the FM exchange coupling between the AF and the FM layer, and the last term represents the Zeeman energy with $M_S = 1.4 \times 10^6$ A/m. The value of B is fixed at 4×10^{-11} J/m to be with the experimental results for the EB field and the degree of asymmetry in the first hysteresis loop. The angles α_i, β_i, θ, and φ correspond to the angles between the AF magnetization, AF easy axis, FM magnetization, applied field, and the [100] direction of the MgO substrate, respectively. The easy axes of the MCA for the FM layer are along $\langle 110 \rangle$ as confirmed by our measurements of the magnetic anisotropy at room temperature. The easy axes of the AF grains are distributed randomly [31]. It should be stressed that a uniform easy axis results in the absence of training within the framework of our model. We consider 49 AF grains that are exchange coupled with one single FM domain. The grain sizes are distributed based on the STM topography images with a bimodal log-normal distribution with average diameters of 5.6 nm and 10.0 nm and standard deviations of 6.0 nm and 8.0 nm, respectively. The abundance ratio for the two CoO diameters is about 5:1. After field cooling the

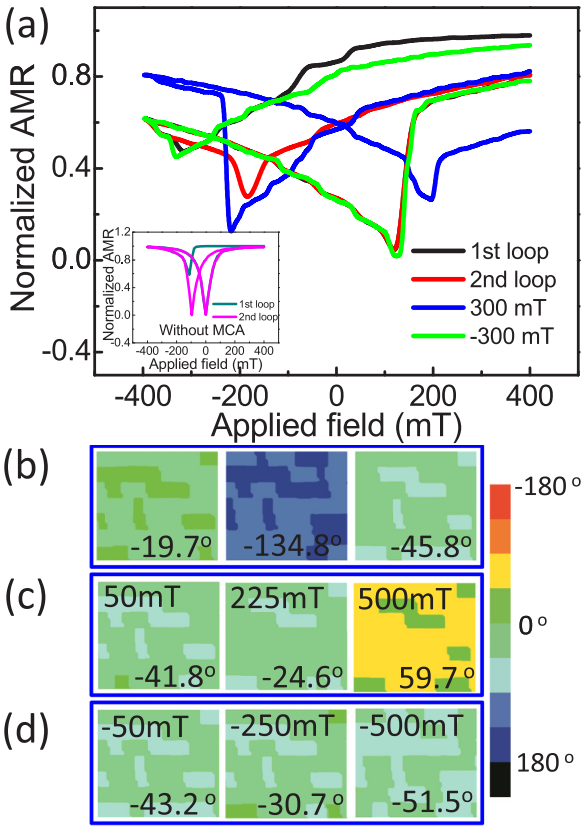

FIG. 3. (Color online) (a) Simulated AMR curves for the untrained, trained, and restored loops after applying perpendicular hysteresis loops with field amplitudes of 300 mT and −300 mT. Inset: simulated AMR curves for the untrained and trained hysteresis loops without MCA. (b) Domain maps of the interfacial AF magnetization after FC, the first reversal, and a complete hysteresis loop. (c),(d) Domain maps of AF magnetization after performing perpendicular hysteresis loops starting from the +90° direction and the −90° direction, respectively. The direction of the average uncompensated magnetization and perpendicular field amplitude are labeled in the lower right and upper left corners, respectively.

magnetization of each of the AF grains is oriented along the easy axis closest to the cooling field. For the distribution, which provides the best agreement with the results of AMR measurements, this results in a total uncompensated magnetization oriented −19.7° away from the FC direction [see the leftmost domain map in Fig. 3(b)]. The magnetization of the FM layer is initially aligned with the cooling field. The magnetization directions of the AF grains and of the single FM domain at different applied fields after FC are determined by minimization of the total energy. When the applied field reaches −400 mT, i.e., when it is opposite to the cooling field after the first magnetization reversal, the average uncompensated magnetization of the AF grains still lags far behind the applied field (−134.8°), as illustrated in the middle domain map in Fig. 3(b). Therefore, the magnetization of the FM layer is also far from saturation due to the MCA and the strong interface coupling between the AF and FM layers. After a complete hysteresis loop the average uncompensated magnetization of the AF grains cannot rotate back to its initial state [the rightmost domain map in Fig. 3(b)], generating a torque on the FM magnetization which favors magnetization rotation passing by the direction perpendicular to the cooling field. In Fig. 3(a) we present the simulated results for the untrained, trained, and restored hysteresis loops for a field amplitude of the perpendicular hysteresis loops of 300 mT and −300 mT, which reproduce well the main trends of the experimental results. From the comparison with the simulated untrained and trained hysteresis loops without MCA [inset of Fig. 3(a)], we conclude that the presence of the MCA results in a less pronounced degree of asymmetry in the untrained hysteresis loop than in the polycrystalline system [19] and also in a survival of the reversal asymmetry after training.

The simulated dependence of the EB field and degree of asymmetry on the perpendicular field amplitude for restored loops and perpendicular loops are presented in Fig. 2(b) and is in qualitative agreement with the experimental results in Fig. 2(a). Based on our simulation, the average uncompensated AF magnetization gradually rotate from negative orientation towards positive orientation with respect to cooling field after performing perpendicular hysteresis loops starting along +90° direction, as illustrated in Fig. 3(c). Consequently, the magnetization reversal process changes from negative rotation sense (magnetization rotation passes by −90° direction) towards positive rotation sense (magnetization rotation passes by +90° direction) [19], and the reversal asymmetry is inverted. We note that the peaks occurring in Fig. 2(b) for the restored EB field and the degree of asymmetry at a field amplitude of about 225 mT correspond to a similar value of the average uncompensated AF magnetization than for the untrained state [compare the leftmost domain map in Fig. 3(b) and the middle domain map in Fig. 3(c)], consistent with the polycrystalline case [19]. On the other hand, the restored average uncompensated AF magnetization approaches the untrained state after applying perpendicular loops starting in the −90° direction with increasing field amplitude [see the first two domain maps in Fig. 3(d)], which results in the partial restoration of the untrained state for a wide range of perpendicular field amplitudes. When further increasing the field amplitude, the direction of the average uncompensated AF magnetization deviates more and more from the untrained state and gets close to the trained state, as illustrated by the rightmost domain map in Fig. 3(d). It should be stressed that for the appropriate perpendicular field amplitudes the simulated restoration of the EB field and of the degree of asymmetry [Fig. 2(b)] becomes much more pronounced than in the experiment [Fig. 2(a)]. This is because we consider only one single FM domain that is exchange coupled with the average uncompensated AF magnetization in a direction corresponding to a negative angle with the cooling field direction, while there possibly also exist FM domains coupled with average uncompensated AF magnetization making a positive angle with the cooling field direction. Therefore, the untrained state can only be partially restored in the experiment. The reversal asymmetry of the perpendicular loop is also directly related to the rotation sense of the FM layer and the orientation of the average uncompensated AF magnetization. A negative rotation sense of the FM magnetization in the hysteresis loop (negative orientated average uncompensated AF magnetization) corresponds to a larger portion of domain wall motion in the descending branch than in the ascending

branch, and vice versa. Hence it is possible to manipulate the reversal asymmetry of an EB system by changing the relative orientation of the average uncompensated AF magnetization. Finally, the occurrence of positive exchange bias in the perpendicular hysteresis loop [see Fig. 2(b)] is due to the fact that the average uncompensated AF magnetization is far away from the applied field direction (with the angle larger than 90°), which favors the FM magnetization to point in the direction opposite to the applied field.

In summary, we demonstrated that due to the presence of magnetocrystalline anisotropy in exchange biased CoO/Co bilayers grown epitaxially on MgO (001), the asymmetry of the magnetization reversal along the field cooling direction survives after training, in contrast to the case of polycrystalline bilayers. Surprisingly, the reversal asymmetry can be inverted by applying a perpendicular hysteresis loop starting from one particular field direction and substantial positive exchange bias appears in the perpendicular loops. The untrained state can be partially restored by applying a perpendicular hysteresis loop starting from the opposite field direction. The microscopic origin is related to the relative orientation of the average uncompensated antiferromagnetic magnetization with respect to the cooling field, which can be modified by applying in-plane perpendicular loops. This way, we establish the possibility to manipulate the magnetization reversal asymmetry resulting from exchange bias.

This work has been supported by the Research Foundation–Flanders (FWO, Belgium), as well as by the Flemish Concerted Research Action program (BOF KU Leuven, project GOA/14/007) and the Flemish Hercules Foundation (project AKUL 09/042).

[1] M. Kiwi, J. Magn. Magn. Mater. **234**, 584 (2001).
[2] J. Nogués and I. K. Schuller, J. Magn. Magn. Mater. **192**, 203 (1999).
[3] F. Radu and H. Zabel, Springer Tracts Modern Phys. **227**, 97 (2007).
[4] J. Nogués, J. Sort, V. Langlais, V. Skumryev, S. Suriñach, J. Muñoz, and M. Baró, Phys. Rep. **422**, 65 (2005).
[5] M. R. Fitzsimmons, P. Yashar, C. Leighton, I. K. Schuller, J. Nogués, C. F. Majkrzak, and J. A. Dura, Phys. Rev. Lett. **84**, 3986 (2000).
[6] M. Gierlings, M. J. Prandolini, H. Fritzsche, M. Gruyters, and D. Riegel, Phys. Rev. B **65**, 092407 (2002).
[7] M. Gruyters and D. Riegel, Phys. Rev. B **63**, 052401 (2000).
[8] S. K. Mishra, F. Radu, H. A. Dürr, and W. Eberhardt, Phys. Rev. Lett. **102**, 177208 (2009).
[9] A. K. Suszka, O. Idigoras, E. Nikulina, A. Chuvilin, and A. Berger, Phys. Rev. Lett. **109**, 177205 (2012).
[10] T. Gredig, I. N. Krivorotov, and E. D. Dahlberg, Phys. Rev. B **74**, 094431 (2006).
[11] T. Gredig, I. Krivorotov, and E. Dahlberg, J. Appl. Phys. **91**, 7760 (2002).
[12] M. Gruyters, J. Appl. Phys. **95**, 2587 (2004).
[13] F. Radu, M. Etzkorn, R. Siebrecht, T. Schmitte, K. Westerholt, and H. Zabel, Phys. Rev. B **67**, 134409 (2003).
[14] J. Camarero, J. Sort, A. Hoffmann, J. M. García-Martín, B. Dieny, R. Miranda, and J. Nogués, Phys. Rev. Lett. **95**, 057204 (2005).
[15] K. Temst, E. Girgis, R. Portugal, H. Loosvelt, E. Popova, M. Van Bael, C. Van Haesendonck, H. Fritzsche, M. Gierlings, L. Leunissen, *et al.*, Eur. Phys. J. B **45**, 261 (2005).
[16] T. Pokhil, R. Chantrell, C. Hou, and E. Singleton, J. Magn. Magn. Mater. **272-276**, E849 (2004).
[17] Z. Y. Liu and S. Adenwalla, Phys. Rev. B **67**, 184423 (2003).
[18] P. Kappenberger, S. Martin, Y. Pellmont, H. J. Hug, J. B. Kortright, O. Hellwig, and E. E. Fullerton, Phys. Rev. Lett. **91**, 267202 (2003).
[19] S. Brems, K. Temst, and C. Van Haesendonck, Phys. Rev. Lett. **99**, 067201 (2007).
[20] C. Leighton, M. R. Fitzsimmons, P. Yashar, A. Hoffmann, J. Nogués, J. Dura, C. F. Majkrzak, and I. K. Schuller, Phys. Rev. Lett. **86**, 4394 (2001).
[21] A. Hoffmann, Phys. Rev. Lett. **93**, 097203 (2004).
[22] E. Fulcomer and S. Charap, J. Appl. Phys. **43**, 4190 (1972).
[23] B. Beckmann, U. Nowak, and K. D. Usadel, Phys. Rev. Lett. **91**, 187201 (2003).
[24] R. Wu, J. Wei, X. Peng, J. Fu, S. Liu, Y. Zhang, Y. Xia, C. Wang, Y. Yang, and J. Yang, Appl. Phys. Lett. **104**, 182403 (2014).
[25] Z. Li, O. Petracic, R. Morales, J. Olamit, X. Batlle, K. Liu, and I. K. Schuller, Phys. Rev. Lett. **96**, 217205 (2006).
[26] S. Brems, D. Buntinx, K. Temst, C. Van Haesendonck, F. Radu, and H. Zabel, Phys. Rev. Lett. **95**, 157202 (2005).
[27] J. Demeter, E. Menéndez, A. Teichert, R. Steitz, D. Paramanik, C. Van Haesendonck, A. Vantomme, and K. Temst, Solid State Commun. **152**, 292 (2012).
[28] Y. Nukaga, M. Ohtake, M. Futamoto, F. Kirino, N. Fujita, and N. Inaba, IEEE Trans. Magn. **45**, 2520 (2009).
[29] F. Radu, A. Westphalen, K. Bröhl, and H. Zabel, J. Phys.: Condens. Matter **18**, L29 (2006).
[30] J. Wu, J. S. Park, W. Kim, E. Arenholz, M. Liberati, A. Scholl, Y. Z. Wu, C. Hwang, and Z. Q. Qiu, Phys. Rev. Lett. **104**, 217204 (2010).
[31] M. S. Lund and C. Leighton, Phys. Rev. B **76**, 104433 (2007).